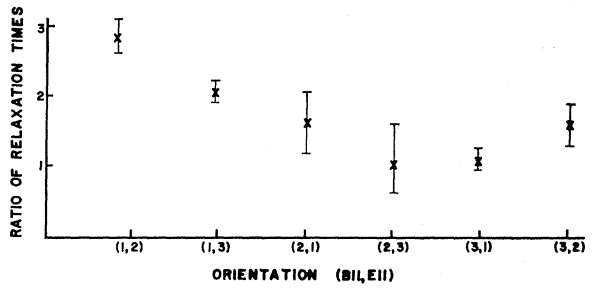

FIG. 8. Normalized ratios of the theoretical relaxation times calculated by Brownell and Hygh to our experimental values. On the X axis, the first number in parentheses refers to the B field direction and the second to the E_{rf} field direction. The binary axis is 1, bisectrix axis 2, and trigonal axis 3. The ratio at (2,3) was taken to be 1.

provide the required percentage of scattering centers and yet preserve electron-hole equality. But the Frenkel defect concentration is sensitive to the prior history of the sample, and we would expect different samples to give different results, especially those prepared in different ways or cycled from room temperature to 4.2°K a different number of times. The good internal agreement in the present experiment and the agreement between our results and McLachlan's results imply that the cause of the relaxation-time values is probably not Frenkel defects.

The present experimental technique is very convenient in comparison with the size-effect and galvanomagnetic[20] methods of determining the relaxation times. In the size-effect method, the resistance is measured in samples at different thicknesses, allowing a determination of $d/V_F\tau$ (where V_F is the Fermi velocity). However, the frequent thermal cycling and the possible strains and dislocations introduced in reducing the size of an already very thin sample make the method subject to error. In the present method, $e^{-d/V\tau}$ is determined in a single sample with one sweep of the magnetic field. In comparison with galvanomagnetic methods, no assumption is made about the Fermi-surface model and no leads are attached to the sample in the present work; thus, it should give a more direct determination of the relaxation times.

ACKNOWLEDGMENTS

We would like to thank Jay Kirschenbaum for his help in the microwave work, and B. Sutherland for useful discussions.

[20] R. N. Zitter, Phys. Rev. **127**, 1471 (1962).

PHYSICAL REVIEW VOLUME 182, NUMBER 2 10 JUNE 1969

Raman Scattering from Solid-State Plasmas

P. M. PLATZMAN
Bell Telephone Laboratories, Murray Hill, New Jersey 07974

AND

N. TZOAR
The City College of The City University of New York, New York, New York 10031

(Received 2 April 1968; revised manuscript received 10 January 1969)

A microscopic calculation of the Raman scattering process in almost transparent semiconductors is presented. The calculation takes into account band structure, phonons, and the collective motions of the conduction electrons. It is based on many-body perturbation theory and is "valid" within the framework of the random-phase approximation. Our results show resonance scattering from the coupled collective modes of the conduction-electron longitudinal-optic-mode system. The detailed effect of the band structure manifests itself in determining the intensity of the resonance lines.

I. INTRODUCTION

THE ever increasing availability of intense monochromatic sources in the infrared has made possible Raman scattering from narrow-band-gap semiconductors. More specifically, successful light scattering experiments have been performed in weakly doped GaAs,[1] InAs, and InSb.[2] An analysis of the data in these three experiments has been based on rather simple theoretical treatment of the light scattering problem.[3,4] The theory is essentially formulated in terms of a single-band model of a semiconductor. The band structure is assumed to be completely characterized by an effective-mass tensor and sometimes by an additional enhancement factor which in an approximate way

[1] A. Mooradian and G. B. Wright, Phys. Rev. Letters **16**, 999 (1966).

[2] R. E. Slusher, C. K. N. Patel, and P. A. Fleury, Phys. Rev. Letters **18**, 530 (1967); C. K. N. Patel and R. E. Slusher, Phys. Rev. (to be published).

[3] P. M. Platzman, Phys. Rev. **139**, A379 (1965); A. L. McWhorter, in *Physics of Quantum Electronics*, edited by P. L. Kelley, B. Lax, and P. E. Tannenwald (McGraw-Hill Book Co., New York, 1966), p. 111.

[4] Y. C. Lee and N. Tzoar, Phys. Rev. **140**, A396 (1965).

takes into account the closeness of the initial laser frequency to the direct band gap in the solid.[5] Phonons are grafted on to the analysis by "adding" their contribution to the dielectric constant to the electron's contribution.[4,6]

Recently, a number of authors have attempted to improve on the earlier formulations of the problem. Wolff,[7] neglecting phonons and using an effective one-band Hamiltonian, has done a microscopic calculation of light scattering which correctly takes into account the generally complicated energy-versus-momentum relationship of the carriers in the conduction band but omits all phonon and explicit interband effects. McWhorter and Argyres[8] and Mooradian and McWhorter[9] have calculated the cross section for light scattering from a real solid with both band structure and phonons. Their calculation is only partially microscopic. This paper will present a microscopic calculation of the Raman scattering process, in almost transparent semiconductors, which takes into account band-structure phonons and the collective motions of the conduction electrons. It is based on many-body perturbation theory and is "valid" within the framework of the random-phase approximation (RPA).

The inelastic or Raman scattering of light from a medium containing mobile carriers (plasmas) provides useful information about the spectrum and nature of the elementary excitations in the medium. In the scattering process, a well-colliminated beam of monochromatic radiation is incident on an almost transparent solid. Subsequently, a small amount of the radiation is scattered into 4π sr. The light which comes off in some fixed direction is then analyzed in a spectrometer. The spectral distribution of the scattered radiation, along with an associated angular distribution, provides the basic information which is contained in this type of experiment.

The scattering (diagramed in Fig. 1) is completely characterized by the quantities $\mathbf{q}=\mathbf{k}_1-\mathbf{k}_2$, the "momentum" transferred to the system, and $\omega=\omega_1-\omega_2$, the "energy" transferred to the system. Here k_2 (k_1) and ω_2 (ω_1) are the final (initial) wave vector and frequency of the scattered (incident) radiation. It is useful to classify the scattering according to the magnitude of $\mathbf{q}$ (fixed scattering angle θ) and then for this fixed $\mathbf{q}$ to analyze the spectrum, i.e., the dependence of scattered light intensity on ω. The momentum (wave vector) transferred to the system, crudely speaking, describes the graininess with which we look at the system spatially. The beam which is undergoing scattering is in effect a microscope with a spatial resolving power which (as for conventional microscopes) is ultimately

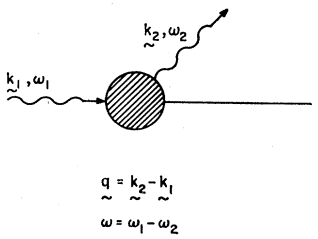

FIG. 1. Diagrammatic representation of the incoherent scattering process. The dashed region represents the plasma, and the two wiggly lines represent the incoming and outgoing photon, respectively.

limited by the wavelength of the incident light. The maximum resolution (smallest distance) occurs for back-scattering. With present laser beams we are able to probe the system to distances of the order of 10^3–10^4 Å, i.e., much larger than typical lattice constants in solids. In insulating or intrinsic semiconducting crystals, this implies that we can only learn something about the *phonon* spectrum very near $q=0$. For the plasma in the conduction band of the solid the characteristics lengths λ_c (the Fermi-Thomas screening length for a degenerate gas) are not very small. Typically they are in the neighborhood of 10^3 Å. This means that although $q\lambda_c<1$ for the solid-state plasma, it is not very much smaller than 1, and we may hope to see effects due to the finite value of $q\lambda_c$.

If we could achieve the condition $q\lambda_c\gg1$, i.e., high resolution, we would get direct information about the electron velocity distribution in the solid.[10,3] Here the scattering takes place from a single electron, i.e., from many electrons incoherently, and the Doppler-shifted frequency of the scattered light is a direct measure of the electron's velocity. When $q\lambda_c<1$ (poor resolution), we are in fact scattering coherently from a large number of carriers and the spectrum primarily reflects the collective motions of the electron gas. We are able, as we shall see, to couple to all collective modes which have a *charge* density associated with them or are themselves coupled indirectly to charge-density fluctuations. In a simple one-component degenerate plasma for a fixed scattering angle, the scattered line is shifted down in frequency from the main line by the plasma frequency, i.e.,[3]

$$\omega^2=\omega_p^2+\tfrac{3}{5}q^2V_F^2. \tag{1}$$

When there are Raman-active phonons in the solid, the situation is more complicated.[1] The longitudinal phonons will couple to the plasmons and the scattered spectrum will show several (hopefully sharp) lines, which reflects the coupling between plasmons and phonons.

The calculations in this paper are restricted to the so-called first-order Raman effect where a single elementary excitation, i.e., phonon, plasmon, or a linear combination, is excited in the scattering process. The

[5] P. A. Wolff, Phys. Rev. Letters **16**, 225 (1966).
[6] B. B. Varga, Phys. Rev. **137**, A1896 (1965).
[7] P. A. Wolff, Phys. Rev. **171**, 436 (1968).
[8] A. L. McWhorter and P. N. Argyres (to be published).
[9] A. Mooradian and A. L. McWhorter, Phys. Rev. Letters **19**, 850 (1967); E. Burstein, A. Pinczuk, and S. Iwasa, Phys. Rev. **157**, 611 (1967).
[10] P. M. Platzman and N. Tzoar, Phys. Rev. **139**, A410 (1965).

semiconductors investigated experimentally all have two atoms per unit cell so that there are three acoustic- and three optic-mode branches in the empty lattice (no doping). Both types of phonons contribute to the first-order Raman effect, but the optic mode, owing to its higher frequency, is easier to resolve and measure, so it has received much more attention than the acoustic mode.[11] In the lattice with carriers in it, it is the longitudinal optic mode which mixes with the plasmon and leads to several interesting effects.[1,6] We will only consider the coupling of the conduction electrons to optic phonons. A consideration of the effect of acoustic phonons on the Raman scattering, conventionally called Brillouin scattering, in the presence of free carriers will be important in an analysis of experiments where the so-called "ion-acoustic" modes are present.[3]

In Sec. II the Hamiltonian for the problem is given and the general expression for cross section is written. In Sec. III, the Raman cross section is expanded as a set of diagrams and the class of diagrams to be summed is discussed. More precisely, we show how the effective-mass approximation arises, how the enhancement factor when the frequency of the light is near the band gap comes in, and how the zeros of the wave number and frequency-dependent dielectric constant will determine the positions of the resonances. Section IV will discuss the zeros of dielectric constant with emphasis on finite q and lifetime effects.

II. FORM OF THE INTERACTION

Raman scattering of photons from a doped semiconductor proceeds via the coupling of the electromagnetic field to the electrons in both valence and conduction bands. In the undoped case, the photons change the vibrational state of the system, i.e., we are left with a single-phonon excitation. The electronic state of the system is left unchanged, since the first electronic excited state is too far removed in energy above the ground state to be excited by the photon. In the doped semiconductor the electronic states form a continuum above the ground state, and the crystal can be left with its electronic state as well as its vibrational state altered.

In order to compute the Raman cross section we must know how the light couples to the electrons, in both the valence and conduction bands of the solids. Since the coupling of the light to the solid is assumed to be very weak, we are only interested in knowing the quantitative nature of this coupling to second order in the electromagnetic field. To this order there are fundamentally two distinct types of interaction which we must consider. The two types correspond to the $-\mathbf{A}^2$ and $\mathbf{p}\cdot\mathbf{A}$ terms obtained in an expansion of the single-electron kinetic-energy operator (schematically)

$$\left(\mathbf{p}-\frac{e}{c}\mathbf{A}\right)^2 \rightarrow \mathbf{p}^2-\frac{e}{c}[\mathbf{p}\cdot\mathbf{A}+\mathbf{A}\cdot\mathbf{p}]+\left(\frac{e}{c}\mathbf{A}\right)^2, \quad (2)$$

where $\mathbf{A}$ is the vector potential of a transverse electromagnetic wave. For the system of n electrons in the solid, the $\mathbf{P}\cdot\mathbf{A}$ type of term may be written[12]

$$H_1=-\frac{e}{m}\sum_{jk}\left(\frac{2\pi}{\omega_k}\right)^{1/2}[a_k e^{i\mathbf{k}\cdot\mathbf{x}_j}+a_k^\dagger e^{-i\mathbf{k}\cdot\mathbf{x}_j}]\mathbf{P}_j\cdot\boldsymbol{\varepsilon}_k. \quad (3)$$

The a_k ($a_k^\dagger$) is the usual annihilation (creation) operator for the photons with polarization vector $\boldsymbol{\varepsilon}_k$. The quantity $\mathbf{P}_j$ ($\mathbf{x}_j$) is the momentum (position) operator of the jth electron. The sum over j is over all electrons both valence and conduction. The operator H_1 has four "different" kinds of matrix elements connecting the ground state of the system to excited states. The four distinct types of matrix elements are shown schematically in Fig. 2. In Fig. 2(a) a photon of momentum $\hbar k_1$ (wiggly line) is annihilated and an electron-hole (solid lines) pair is created having relative momentum $\hbar k_1$. The electron is excited from a filled valence band v to an empty-conduction-band state c. In Fig. 2(b) a pair which is present annihilates and absorbs a photon. Figures 2(c) and 2(d) show the same process, but in this case we have created an electron-hole pair in the partially filled conduction band, i.e., we have used the intra- rather then the interband matrix element of $\mathbf{P}\cdot\mathbf{A}$. This type of process does not exist for the insulating case. One can show[13] that the intraband matrix elements of $\mathbf{P}\cdot\mathbf{A}$ are small relative to the interband pieces in the ratio $r\equiv k_1/k_l$, where k_l is a reciprocal-lattice vector. We neglect them. The diagrams in Fig. 2 have their Hermitian counterparts. The only change is that a photon is created rather than destroyed.

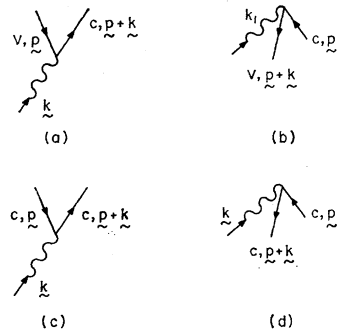

FIG. 2. (a) and (b) represent the annihilation of a photon with pair creation and annihilation, respectively. Here the pair describe the excitation of an electron from the valence band into the conduction band. (c) and (d) describe the same process for an intraband (conduction) transition.

[11] R. Loudon, Proc. Roy. Soc. (London) **275**, 218 (1963).

[12] We use units in which $\hbar=c=1$ and we consider a unit volume of material so that all factors of V, the volume of the system, are absent.

[13] P. M. Platzman and N. Tzoar, Phys. Rev. **136**, A11 (1964).

The $\mathbf{A}^2$ coupling term may be simply written as

$$H_2=\frac{e^2}{m}\sum_j\sum_{k\neq q}[a_k e^{i\mathbf{k}\cdot\mathbf{x}_j}+a_k^\dagger e^{-i\mathbf{k}\cdot\mathbf{x}_j}]\boldsymbol{\varepsilon}_k\cdot\boldsymbol{\varepsilon}_q$$
$$\times[a_q^\dagger e^{-i\mathbf{q}\cdot\mathbf{x}_j}+a_q e^{+i\mathbf{q}\cdot\mathbf{x}_j}]\left[\frac{2\pi}{\omega_q}\right]^{1/2}\left[\frac{2\pi}{\omega_k}\right]^{1/2}. \quad (4)$$

H_2 has the matrix elements shown diagrammatically in Fig. 3. In this case two photons are involved (A^2). The initial photon is destroyed, the final one created, and a pair is created all at a single vertex. The pair may have a hole, as for the matrix elements of H_1, either in the valence band [Fig. 3(a)] or in the partially filled conduction band [Fig. 3(b)]. However, unlike the linear matrix elements, the situation is reversed. Only the *intraband* matrix element of A^2 is important, i.e., we keep only Fig. 3(b), where the A^2 term creates an electron-hole pair in the partially filled conduction band.[14] The ratio of the matrix elements in Fig. 3(a) to those in Fig. 3(b) is roughly of order r as in Fig. 2. The matrix element of A^2 which is large in the doped crystal is absent in the pure crystal.

There is an additioinal mechansm by which the light couples directly to the phonons. This coupling is generally overlooked but it is important for understanding, from a microscopic point of view, the frequency dependence of the scattering cross section. This mechanism exists because of the fact that the electrons will adiabatically follow [Born-Oppenheimer approximation (BOA)] the motion of the ions. Its revelance to the Raman process and a discussion of its origin are contained in the Appendix.

The light primarily interacts with the medium by producing electron-hole pairs. These excited electrons couple to modes of the crystal, to the phonons, and to one another by means of Coulomb and phonon interaction effects, and they also couple to impurities which are present.[15] This calculation will assume that both the Coulomb and phonon couplings are weak. We will keep terms in a perturbation expansion of the cross section which are of leading order in the Coulomb interaction

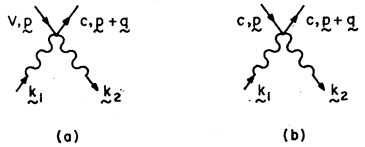

FIG. 3. Schematic description of the matrix element for Raman scattering using the A^2 term of the Hamiltonian. Here the incoming photon $\mathbf{k}_1$ is scattered into the outgoing photon $\mathbf{k}_2$ via a pair (electron-hole) excitation.

[14] For a discussion of this point see any standard book on band structure, for example, J. Callaway, *Energy Band Theory* (Academic Press Inc., New York, 1964).

[15] We neglect any explicit coupling to impurities. In sufficiently pure materials, this coupling is unimportant. It will be included, when necessary, by using a phenomenological relaxation time.

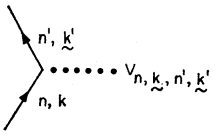

FIG. 4. Schematic description for electron scattering via interaction with a phonon (dotted line).

among the conduction electrons. We will only keep the first-order terms in the electron-phonon coupling and we neglect entirely any Coulomb interaction among the valence electrons. This set of approximations is "equivalent" to the usual RPA. Although it does neglect any "explicit" electron-electron or electron-phonon effects, it does systematically take into account the self-consistent field due to the coupled electron-phonon density fluctuations.

The assumption of a weak Coulomb interaction between conduction electrons is a reasonably good one. The expansion parameter in this case is the parameter r_s, which is roughly the average potential over the average kinetic energy of the conduction electrons. In a typical narrow-band semiconductor like GaAs, with a carrier concentration of 10^{18}, $r_s\cong 0.3$. The neglect of any Coulomb interaction effects among the valence electrons has no *a priori* justification. In some sense it is equivalent to the small r_s approximation for the electrons in the conduction band of the crystal.

The important physical point to make is that we are not interested in the dynamics of the electrons in the valence band. They are in a dynamical sense frozen out of the problem. They do, however, play an important role in the calculation. It is the valence electrons which "produce" the effective Hartree-Fock (pseudo-) potential which leads to the band structure. It is the valence electrons which modify the effective interaction between two static charges in the conduction band, i.e., the Coulomb law of force is $e^2/\epsilon_\infty r$; ϵ_∞ being in the neighborhood of 10 for most narrow-band-gap materials. In addition, the valence electrons provide us with an important indirect mechanism for the coupling of the light to the phonons and to the conduction electrons. We make "no" attempt to treat the entire problem within a many-body perturbation picture but merely treat the conduction electron from this point of view. The many-body aspects of the valence band are buried in ϵ_∞, the measured phonon frequencies, and interband matrix elements (which are never computed) of the momentum operator.

Having discussed how the light interacts with the electrons, we must next consider the coupling of the electrons to the phonons in the medium. There are two distinct types of optic-phonon-mode electron coupling in semiconductors such as GaAs. The first, the so-called Frölich coupling, is fundamentally an interaction of the electrons with the charge of the optic-mode vibrations of a polar lattice. This kind of interaction is displayed pictorially in Fig. 4. The dotted line is a phonon. The interaction vertex $V_{n,\mathbf{k},n',\mathbf{k}'}$ describes the scattering

of an electron (hole) from a state specified by the band index n and crystal momentum $\mathbf{k}$ to another specified by n' and $\mathbf{k}'\equiv\mathbf{k}+\mathbf{q}$.

$$V_{n,\mathbf{k},n',\mathbf{k}'}{}^{F}=\frac{ie}{q}\left(\frac{1}{\epsilon_\infty}-\frac{1}{\epsilon_0}\right)^{1/2}(2\pi\omega_0)^{1/2}N_{\alpha,\beta}\,, \tag{5}$$

with

$$\begin{aligned} N_{\alpha,\beta}&=1, && n=n'\\ &=qp_{\beta,\alpha}{}^{q}/m(E_\beta-E_\alpha), && n\neq n'. \end{aligned} \tag{6}$$

Here ω_0 is the optical-mode phonon frequency at $q=0$, and $E_{n,\mathbf{k}}$ is a one-electron energy. The index α is equivalent to n and $\mathbf{k}$. The quantity $p_{\beta,\alpha}{}^{q}$ is the matrix element of $\mathbf{P}$ in the direction q, i.e.,

$$p_{\beta,\alpha}{}^{q}\equiv\langle\beta|\mathbf{P}\cdot\hat{q}|\alpha\rangle.$$

The interband matrix elements $n\neq n'$ of the Fröhlich coupling are much smaller than the intraband pieces in the ratio r. For a number of important intraband processes the matrix elements almost cancel and we shall see that we must include the contribution from the interband pieces as well.

The second important type of electron-phonon coupling is the so-called deformation-potential coupling.[11] This coupling, like the Fröhlich coupling, leads to a scattering of electrons or holes. The graphic representation of the scattering process is given in Fig. 4. The corresponding matrix element is[11]

$$V_{\alpha,\beta}{}^{D}=\Xi_{\alpha,\beta}{}^{i}(1/2MN\omega_0)^{1/2}k_l\,, \tag{7}$$

where $\Xi_{\alpha,\beta}{}^{i}$ is the deformation potential, M is the mean ion mass, N is the total number of atoms in the sample, and the superscript i specifies the polarization vector $(\xi_{0q}{}^{i})$ of the phonons.

In a typical narrow-band-gap semiconductor $\Xi_{\alpha,\beta}{}^{i}\cong 5$ eV and $\hbar\omega_0\cong 0.01$ eV. Using these parameters, it is possible to show that $|V^D/(V^F)_{\text{intraband}}|\cong r$, i.e., the deformation potential is small compared to the intraband Fröhlich piece but comparable in magnitude with the interband part of the Fröhlich coupling.

III. CALCULATION OF THE CROSS SECTION

A. No Phonons

Although the Raman cross section can be directly evaluated for the complete system of phonons and conduction electrons, it is useful to consider some limiting cases separately. We will begin by neglecting all phonon effects, i.e., we put the conduction and valence electrons into a rigid lattice. This approximation, although not valid when the "phonon" and "plasmon" frequencies are close together, will give us a clear picture of the origin of the effective one-band Hamiltonian, its validity, and its limitations. This effective one-band Hamiltonian has been used by several authors[3] to compute the light scattering cross sections from semiconducting crystals. Wolff[5] has "derived" the effective one-band Hamiltonian in the absence of any cooperative or plasmalike effects.

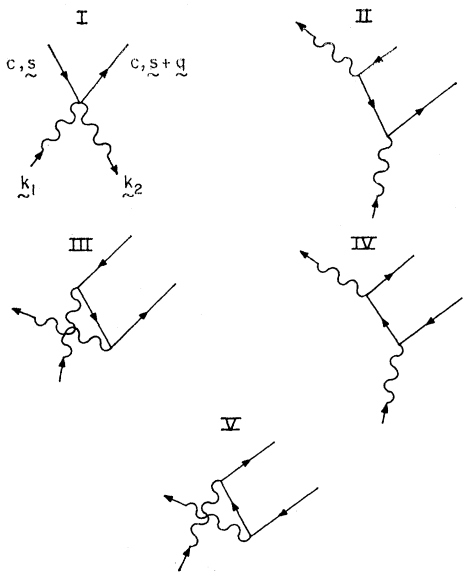

FIG. 5. Raman scattering to zeroth order in the Coulomb interaction among the electrons.

To zeroth order in the Coulomb interaction, we must evaluate the five diagrams shown in Fig. 5. Diagram I is the contribution from H_2. Diagram III is simply the crossed version of diagram II, and its contribution is obtained from its uncrossed counterpart by letting $\mathbf{k}_1\leftrightarrow\mathbf{k}_2$, $\omega_1\leftrightarrow-\omega_2$, and $\mathbf{e}_1\leftrightarrow\mathbf{e}_2$. This operation is called "crossing" and will be designated by the symbol X. In diagrams IV and V, the electron and hole final states have been interchanged. Apart from a numerical factor, the matrix element for the sum of the five lowest-order diagrams in Fig. 5 may be written

$$M^0=e_\mu{}^1e_\nu{}^2A_{\mu\nu}(s)\,, \tag{8}$$

where

$$mA_{\mu\nu}(s)\equiv\delta_{\mu\nu}+\Gamma_{\mu\nu}(s,\omega_1,\omega_2,k_1,k_2)\,, \tag{9}$$

and

$$\Gamma_{\mu\nu}=\frac{1}{m}\left\{\sum_{n\neq c}\frac{\langle c,s-q|P_\nu|n,s-k_1\rangle\langle n,s-k_1|P_\mu|c,s\rangle}{\epsilon_{c,s}-\epsilon_{n,s-k}-\omega_1}+X\right\}. \tag{10}$$

The quantity $\epsilon_{n,k}$ is the one-electron energy in the band n with crystal momentum $\mathbf{k}$. All the energies are measured from the bottom of the conduction band. The sum over n is over *all* band indices with $n\neq c$.

If E_g is the gap energy in the undoped crystal, the leading term in a low-frequency $(\hbar\omega_{1,2}/E_g\to 0)$, long-wavelength $(k_{1,2}/k_l\to 0)$ expansion of $A_{\alpha\beta}$ is simply related to the conduction-electron energy-momentum relation. In this limit, heretofore called the "zero limit,"

$$A_{\alpha\beta}=(\partial^2\epsilon^c/\partial p_\mu\partial p_\nu)_{p=s}. \tag{11}$$

For a simple parabolic band $A_{\alpha\beta}\equiv\mu_{\alpha\beta}$, the inverse effective-mass tensor, and

$$M^0=\mathbf{e}_1\cdot\boldsymbol{\mu}\cdot\mathbf{e}_2 \tag{12}$$

is the matrix element which one uses in a simple effective-mass approximation, to one-particle Thompson scattering in a crystal.[3,4] This approximation, Eq. (12), clearly neglects all cooperative effects.

Setting k_1 and k_2 equal to zero is a good approximation. The wave vector of the light is, in most experimental cases, small compared to k_l. Setting ω_1 and ω_2 equal to zero is not a very good approximation, since the frequency of the light can be in the neighborhood of the energy gap. It is clear from Eq. (10) that near the gap the matrix element is roughly enhanced by a factor $E_g/(E_g+2\epsilon_F-\hbar\omega_{1,2})$ and the cross section by the square of this factor.

In order to include cooperative effects in a calculation of the scattering cross section, we must go to higher order in the Coulomb interaction between particles in the conduction band. We will do the leading-order term (first-order) and then show how the required sum of terms, i.e., the effective screening of the interaction, is simply included. To the first order in the Coulomb interaction between conduction electrons, we must evaluate 10 different diagrams shown in Fig. 6. Four diagrams are just the crossed version of their predecessors, so that we only need to evaluate six diagrams. These are conveniently evaluated in pairs. Diagrams I and II are the first-order correction terms arising from the A^2 piece. The sum of these two terms is given by

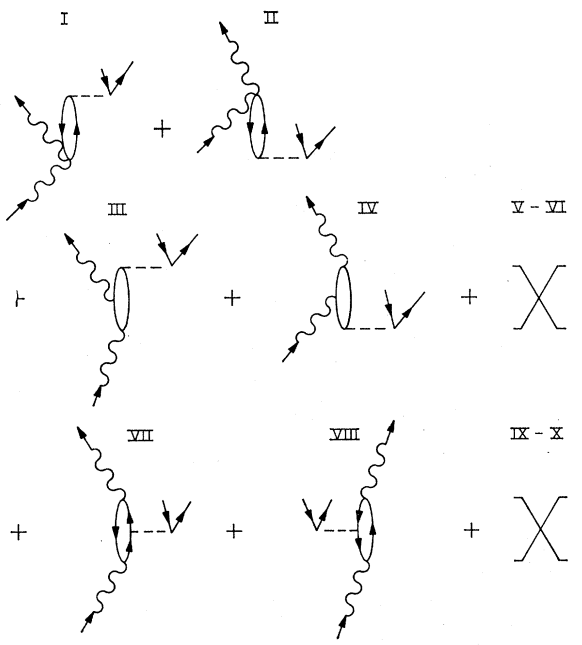

FIG. 6. That portion of the Raman scattering matrix element which is first-order in the Coulomb interaction among the electrons.

FIG. 7. Diagrammatic representation of the screened Coulomb interaction; here $\varphi_q\rightarrow\varphi_q/\epsilon(q,\omega)$.

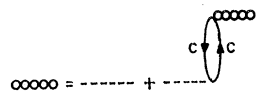

$M^{(1)}$, where

$$M^{(1)}=\delta_{\mu\nu}\varphi_q Q_e(q,\omega), \tag{13}$$

and

$$Q_e(q,\omega)=\int\frac{f_{p-q}^{-}-f_p^{-}}{\epsilon_{p-q}{}^c-\epsilon_p{}^c-\omega-i\delta}\frac{d^3p}{(2\pi)^3}. \tag{14}$$

The function f_p^- is the Fermi function and Q_e is the RPA polarizability of the electron gas. The quantity $\varphi_q=4\pi e^2/q^2\epsilon_\infty$ is the Fourier transform of the Coulomb interaction in the crystal. It is simply the matrix element associated with the horizontal dashed line in Fig. 6.

If there were no interband effects, i.e., a "free"-electron gas, then diagrams I and II in Fig. 6 would be the only contribution to $M^{(1)}$. In this case, we would combine $M^{(1)}$ with the $\delta_{\mu\nu}$ piece in Eq. (9). Adding these two pieces up, summing over final states which conserve energy, and averaging over an initial ensemble at a temperature $\beta=1/kT$, we get for the differential cross section

$$\left.\frac{d\sigma}{d\omega\,d\Omega}\right|_{A^2}=r_0^2(\mathbf{e}_1\cdot\mathbf{e}_2)^2\frac{\omega_1}{\omega_2}\sum_s f_s^{-}f_{s+q}{}^{+}\delta(\epsilon_{s+q}-\epsilon_s-\omega)\times|1+\varphi_q Q_e(q,\omega)|^2, \tag{15}$$

where

$$r_0=e^2/mc^2$$

and $f^+\equiv1-f^-$. Since

$$\sum_s f_s^{-}f_{s+q}{}^{+}\delta(\epsilon_{s+q}-\epsilon_s-\omega)=-\frac{1}{\pi}\frac{1}{1-e^{-\beta\omega}}\,\mathrm{Im}Q_e(q\omega), \tag{16}$$

we find that

$$\left(\frac{d\sigma}{d\omega\,d\Omega}\right)_{A^2}=-\frac{1}{\pi}\frac{r_0^2(\mathbf{e}_1\cdot\mathbf{e}_2)^2}{1-e^{-\beta\omega}}\times\mathrm{Im}Q_e(q,\omega)|1+\varphi_q Q_e(q,\omega)|^2. \tag{17}$$

The screening, or cooperative, effects are easily inserted into Eq. (17). We merely replace φ_q by $\varphi_q/\epsilon(q,\omega)$.[16] The quantity $\epsilon(q,\omega)=1-\varphi_q Q_e(q,\omega)$ is the wave number and frequency-dependent dielectric constant for the electron gas. This replacement is equivalent to changing the "bare" Coulomb line in Fig. 6 into a dressed Coulomb line, pictorially represented by the infinite set of diagrams shown in Fig. 7. The bubbles in this string of diagrams all represent an excited electron-hole pair in the *conduction* band. Replacing the bare interaction by a screened interaction is equivalent to the RPA.[16] It is the only "many-body" effect to be

[16] For a discussion of this point, see, for example, D. Pines and P. Nozières, *Quantum Liquids* (W. A. Benjamin, Inc., New York, 1966), Chap. IV.

included in this calculation. Inserting $\epsilon(q,\omega)$ into Eq. (17), we find

$$\left.\frac{d\sigma}{d\omega\, d\Omega}\right|_{A^2}=\frac{1}{(\pi)}\frac{r_0^2(\mathbf{e}_1\cdot\mathbf{e}_2)^2}{1-e^{-\beta\omega}}\frac{\mathrm{Im}Q_e(q,\omega)}{|\epsilon(q,\omega)|^2}, \tag{18}$$

a well-known result.[3,4,9]

Let us go back and pick up the remaining diagrams in Fig. 6. Diagrams III–VI give[17]

$$M^{\mathrm{III-VI}}\sim\varphi_q\sum_p\Gamma_{\mu\nu}(p,\omega,k_1,k_2)\frac{f_{p-q}^{-}-f_p^{-}}{\epsilon_{p-q}{}^c-\epsilon_p{}^c-\omega-i\delta}$$
$$+\varphi_q\sum_p f_{p-q}{}^{+}f_p^{-}\left[\frac{\langle p_\mu\rangle\langle p_\nu\rangle}{m\Delta_1\Delta_2}+X\right], \tag{19}$$

where

$$\Delta_1=E_g+\epsilon_{p-k_1}{}^v+\epsilon_p{}^c-\omega_1,$$
$$\Delta_2=E_g+\epsilon_{p-k_1}{}^v+\epsilon_{p-q}{}^c-\omega_2. \tag{20}$$

Diagrams VII–X yield

$$M^{\mathrm{VII-X}}\sim-\varphi_q\sum_p f_{p+q}{}^{+}f_p^{-}\left[\frac{\langle p_\mu\rangle\langle p_\nu\rangle}{m\Delta_1\Delta_2}+X\right]+\varphi_q\mathcal{E}_{\mu\nu}, \tag{21}$$

where $\mathcal{E}_{\mu\nu}$ is a small quantity and is given by

$$\mathcal{E}_{\mu\nu}=\sum_p f_p{}^{+}\frac{[\epsilon_{p-q}{}^c-\epsilon_p{}^c+\epsilon_{p-k_1}{}^v-\epsilon_{p-k_2}{}^v]\langle p_\nu\rangle\langle p_\mu\rangle}{\Delta_1\Delta_2\Delta_3 m}+X, \tag{22}$$

with

$$\Delta_3=E_g+\epsilon_p{}^c+\epsilon_{p-k_2}{}^v-\omega_2. \tag{23}$$

The exact form of $\mathcal{E}_{\mu\nu}$ is unimportant. Its order of magnitude is given by

$$|\mathcal{E}_{\mu\nu}|\cong\sum_p f_p{}^{+}\frac{q^2p^2}{m^2\Delta^4}\frac{\langle p_\mu\rangle\langle p_\nu\rangle}{m}, \tag{24}$$

with Δ a denominator of the form given in Eq. (20). The quantity $(4\pi e^2/q\epsilon_\infty)\mathcal{E}_{\mu\nu}\equiv C_{\mu\nu}$ is to a good approximation a constant independent of $\mathbf{k}_1$, $\mathbf{k}_2$, ω_1, and ω_2 depending only on the band structure of the solid. In a cubic crystal $\mathcal{E}_{\mu\nu}\equiv\mathcal{E}\delta_{\mu\nu}$.

Combining Eq. (19) with Eq. (21), we find that the total contribution to first order in the Coulomb interaction is

$$M^{(1)}\sim\varphi_q\left[\sum_p mA_{\mu\nu}(p)\frac{f_{p-q}^{-}-f_p^{-}}{\epsilon_{p-q}{}^c-\epsilon_p{}^c-\omega-i\delta}+\mathcal{E}_{\mu\nu}\right]. \tag{25}$$

In the "zero limit," $A_{\mu\nu}$ is the second derivative of energy with respect to momentum [see Eq. (11)]. For a simple parabolic band, it is a constant, $(1/m^*)\delta_{\mu\nu}$, which may be taken out of the summation over p. In this approximation the two terms $M^0+M^{(1)}$ are

$$M^{(0)}+M^{(1)}=(e_\mu{}^1e_\nu{}^2/m^*)$$
$$\times\{\delta_{\mu\nu}+\varphi_q[Q_e(q,\omega)\delta_{\mu\nu}+(m^*/m)\mathcal{E}_{\mu\nu}]\}. \tag{26}$$

We may now, as we did in Eq. (18), put in the collective effects by simply replacing

$$\varphi_q[Q_e(q,\omega)\delta_{\mu\nu}+(m^*/m)\mathcal{E}_{\mu\nu}]\rightarrow$$
$$\frac{\varphi_q[Q_e(q,\omega)+(m^*/m)\mathcal{E}_{\mu\nu}]}{\epsilon(q,\omega)}. \tag{27}$$

The total matrix element for light scattering in this approximation (parabolic bands, no phonons) is given by

$$M^T\sim\frac{e_\mu{}^1e_\nu{}^2}{m^*}\left[\delta_{\mu\nu}+\frac{\varphi_q[Q_e(q,\omega)\delta_{\mu\nu}+(m^*/m)\mathcal{E}_{\mu\nu}]}{1-\varphi_qQ_e(q,\omega)}\right]$$
$$\sim e_\mu{}^1e_\nu{}^2\frac{\delta_{\mu\nu}+(m^*/m)C_{\mu\nu}}{1-\varphi_qQ_e(q,\omega)}. \tag{28}$$

Equation (28) has several simple but interesting features in the limit $q\rightarrow 0$. Let qV_F/ω approach zero. In this limit, $\varphi_qQ_e(q,\omega)\rightarrow-\omega_p{}^2/\omega^2$. There is, as one would expect, a resonance in the matrix element, and therefore in the cross section, at $\omega=\omega_p$. It is well known[9,11] that within the framework of the one-band model the area under the plasma line, at zero temperature, i.e., the total cross section per unit solid angle per particle, is given by[3,18]

$$\frac{d\sigma}{d\Omega}=(\mathbf{e}_1\cdot\mathbf{e}_2)^2\left(\frac{e^2}{m^*c^2}\right)^2\frac{\omega_1}{\omega_2}\left(\frac{q}{q_{\mathrm{sc}}}\right)^2\frac{\omega_p}{2E_F}, \tag{29}$$

with $q_{\mathrm{sc}}=(\sqrt{\frac{3}{2}})(\omega_p/V_F)$. In the multiple-band model, the cross section given by Eq. (29) is multiplied by a factor of $(1+C)^2$, where $C\sim C_{\mu\nu}$.

In the neighborhood of the central line where $\omega/qV_F\rightarrow 0$ and $\varphi_qQ_e(q,\omega)\rightarrow(q_{\mathrm{sc}}/q)^2\gg 1$, it is evident from Eq. (28) that the cross section in the central line is suppressed relative to the plasmon contribution by a factor $(q/q_{\mathrm{sc}})^4$. In this "parabolic case" it is the cancellation between the $\varphi_qQ_e(q,\omega)$ in the numerator with the same quantity in the denominator of Eq. (28) which leads to the suppression. The light scattering cross section, in the long-wavelength limit from a system with parabolic bands, is only weakly dependent on the single-particle properties of the plasma. The total cross section under this weak central line is multiplied, as is Eq. (9), by a numerical band-structure-dependent factor $(1+C)^2$ which is outside the one-band model.

Wolff[2] has pointed out that if we relax the parabolic band approximation, i.e., if we allow $A_{\mu\nu}(p)$ to be a

[17] In order to keep the notation simplified we specialize to the case of a two-band model. Electrons have a positive energy $\epsilon_p{}^c$ and holes a positive energy $\epsilon_p{}^v$. The direct band gap is E_g.

[18] For $\omega/qv_F>1$ the $\mathrm{Im}Q_e(q,\omega)$ in the RPA at zero temperature is entirely due to collisions with the lattice and with phonons. The area under the line, assuming that collisions are finite, is independent of the collisions.

function of p in the zero-frequency zero-wave-vector limit for the light, then the behavior of the scattering cross section in the neighborhood of the "central" line is drastically changed.[7] There is no longer a cancellation of the polarizability in the numerator of Eq. (21) with the denominator polarizability and the single-particle-like aspects of the scattering are enhanced. For small q in the neighborhood of the central line in the nonparabolic case we may neglect C. The cross section in this case becomes

$$\frac{d\sigma}{d\omega\, d\Omega}=\left(\frac{e^2}{mc^2}\right)^2 e_\mu{}^1 e_\nu{}^2 \frac{\omega_1}{\omega_2}\sum_s f_s{}^- f_{s+q}{}^+ \delta(\epsilon_{s+q}-\epsilon_s-\omega) \times\left|A_{\mu\nu}(s)+\frac{\varphi_q Q_{\mu\nu}(q,\omega)}{1-\varphi_q Q_e(q,\omega)}\right|^2, \quad (30)$$

with

$$Q_{\mu\nu}=\sum_p \frac{A_{\mu\nu}(p)(f_{p-q}{}^- - f_p{}^-)}{\epsilon_{p-q}{}^c-\epsilon_p{}^c-\omega-i\epsilon}. \quad (31)$$

Equations (30) and (31) are identical to Wolff's results [see Eqs. (19), (22), (23), and (26) of Ref. 7] which were arrived at using an effective one-band Hamiltonian with a nonparabolic energy-momentum relation of the form $E(P)=P^2/2m^*+(P^4/m^{*2})E_g$. This is equivalent to an $A_{\mu\nu}(P)$ of the form

$$m^* A_{\mu\nu}(P)=\delta_{\mu\nu}[1-(P^2/m^*)E_G]-2(P_\mu P_\nu/m^*)E_G. \quad (32)$$

The discussion here may be considered a justification for the use of the effective one-band Hamiltonian in the "zero" limit. Strictly speaking, it is only valid in the single-particle regime where C may be neglected. In the cooperative regime, the absolute intensity is *not* given correctly by the effective one-band Hamiltonian.

B. No Conduction Electrons

Loudon[11] has discussed the problem of the Raman scattering of light from an empty lattice. In this section we will repeat, within the framework of the present theoretical formulation, the bare bones of this calculation. This brief review will enable us to make contact with Loudon's well-known results and it will provide us with a springboard for extracting the scattering cross section for the coupled electron-phonon system. It also allows us to make an essential point relating to the frequency dependence of the Raman cross section. This point has been treated incorrectly or ignored entirely in the literature.

The complete content of the empty lattice calculation, as done by Loudon, is contained in the Feynman diagram shown in Fig. 8. In this diagram no attention is paid to time order or to the difference between crossed and uncrossed photon pieces. Topologically the Feynman diagram is equivalent to the sum of the last eight diagrams shown in Fig. 6. Its contribution is different only insofar as the shaded vertex differs and the final

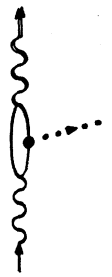

FIG. 8. Feynman diagram representing the most important process in the Raman scattering of light from an insulator. The dashed line is a phonon and the shaded vertex may be either a Frölich or deformation-potential coupling.

state (dashed line) is a phonon. The vertex is either a V^D [Eq. (7)] or a V^F [Eq. (5)]. The matrix element with a deformation-potential coupling at the vertex is proportional to Loudon's $R_{\mu\nu}{}^i$:

$$M^D=e_\mu{}^1 e_\nu{}^2 \frac{\xi_{0q}{}^i k_l R_{\mu\nu}{}^i}{m}\left(\frac{1}{2MN\omega_0}\right)^{1/2}, \quad (33)$$

with

$$R_{\mu\nu}{}^i=\sum_{\substack{n' \text{ empty}\\ n \text{ full}\\ n'' \text{ full}}}\left[\frac{\langle n''|P_\nu|n\rangle\langle n|P_\mu|n'\rangle\Xi_{n''n}{}^i}{\Delta_1\Delta_2} +\text{seven terms}\right]. \quad (34)$$

The first term in the sum of eight terms, in Eq. (34), corresponds to a definite time ordering of the various external lines in Fig. 8. This time ordering is shown in Fig. 6, diagram III. The only essential difference between Eq. (34) and the appropriate piece of Eq. (19) is that we now have a deformation potential at the vertex instead of a Coulomb interaction.

Similarly, the contribution to the matrix element for Fröhlich coupling is

$$M^F=(e_\mu{}^1 e_\nu{}^2 q V_q/m^2)P_{\mu\nu}{}^q, \quad (35)$$

where

$$V_q=\frac{ie}{q}\left(\frac{1}{\epsilon_\infty}-\frac{1}{\epsilon_0}\right)^{1/2}(2\pi\omega_0)^{1/2} \quad (36)$$

and the quantity $P_{\mu\nu}{}^q$ is identical with that defined by Loudon [Eq. (39) of Ref. 11], i.e.,

$$P_{\mu\nu}{}^q=\sum_{n,n',n''}\left[\frac{\langle n''|P_\nu|n\rangle\langle n|P_\mu|n'\rangle\langle n|P^q|n'\rangle}{\Delta_1\Delta_2(\Delta_2+\omega)} +\text{seven terms}\right]. \quad (37)$$

It is important to note that all of the matrix elements of $\mathbf{p}$ in Eq. (37) are interband. The diagrams which correspond to the specific time order shown in Fig. 6 (diagrams VII-X), which do have intraband matrix elements of the Fröhlich coupling, cancel in pairs with one another as shown in Fig. 9. This cancellation is exact when one neglects the k dependence (k_1,k_2) of the electronic energies in the intermediate states. The cancel-

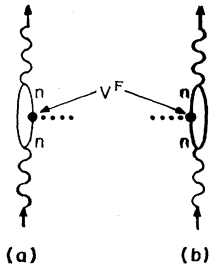

FIG. 9. Pair of time-ordered diagrams which cancel in the long-wavelength limit. The phonon vertex is pure intraband Frölich coupling.

lation implies that it is only the interband matrix elements of the Fröhlich coupling which contribute to the scattering in the undoped crystal. These interband matrix elements are to be identified with the electro-optic coefficient.[11]

At this juncture it is appropriate to examine the frequency dependence of $R_{\mu\nu}{}^{i}$ and $P_{\mu\nu}{}^{q}$. We are particularly interested in the implications of the sum rule proved in the Appendix. The sum rule is nothing but a simple generalization of the well-known f sum rule. It states that the Raman scattering from insulating crystals to arbitrary order in the phonon coupling will go like $(\hbar\omega/E_B)^4$. Here E_B is a typical bandwidth energy, characteristically of the order of a few eV in most materials.

This sum rule is "true" regardless of the number of phonons excited, the strength of the electron-phonon coupling, or the band structure of the solid. All that is required is that the final state of the crystal differ in energy from the initial state by an amount small compared to typical electron energies in the crystal, and that the wave function of the valence electrons be localized over distances small compared to the wavelength of the light [i.e., $(\hbar qc/E_G)\ll 1$]. These conditions are both very well satisfied.

The sum rule comes about because of the cancellation of the A^2 and $\mathbf{P}\cdot\mathbf{A}$ pieces in the general expression for the Raman scattering amplitude [see Eqs. (A1) and (A5)]. The proof does not depend on an explicit perturbation and calculation of the two terms. Equations (34) and (37) for $R_{\mu\nu}{}^{i}$ and $P_{\mu\nu}{}^{q}$ are "approximate" expressions for the $\mathbf{P}\cdot\mathbf{A}$ piece. Both expressions, aside from a simple coupling-constant factor, have the same structure. It is in fact clear from Eqs. (34) and (37) that as $\omega_{1,2}\to 0$, $R_{\mu\nu}{}^{i}$ and $P_{\mu\nu}{}^{q}$ both approach a constant and do not go like $\omega_1{}^2$. It is the contribution due to the direct coupling of the A^2 piece to the phonons which will cancel the constant piece and lead to an $\omega_1{}^2$ dependence of the cross section. We have neglected entirely the A^2 term.

The sum rule presented in the Appendix suggests that the correct procedure for evaluating all matrix elements involved in the scattering is to use a set of electronic basis functions which move with the ions, i.e., the wave function in the distorted crystal. We have incorrectly neglected the A^2 term because we have taken as our basis electronic wave functions tied to fixed lattice points, and assumed that the final and initial states differ only in the nuclear coordinate (phonon) portion of the wave function. If we had used a basis set tied to the ionic coordinates, then the A^2 term would contribute since the final and initial electronic states would parametrically involve the nuclear coordinates. Unfortunately, the electronic wave functions in the distorted crystal are not easily obtainable. The matrix elements of $\mathbf{P}$ in $R_{\mu\nu}{}^{i}$ and $P_{\mu\nu}{}^{q}$ should also be evaluated in the distorted lattice. However, it is clear from the structure of Eq. (34) or Eq. (37) that taking the matrix elements in the undistorted lattice for the $\mathbf{P}\cdot\mathbf{A}$ piece is indeed a *good* approximation. The point is simply that the distortion of the lattice takes place on a very large scale: $q/k_l\ll 1$. The interband matrix elements of $\mathbf{P}\cdot\mathbf{A}$ are short-range in character and the slight distortion of the lattice is unimportant. For the A^2 piece the entire matrix element is long-range in character, i.e., $A^2\sim\sum e^{i\mathbf{q}\cdot\mathbf{x}_i}$, so the distortion is crucial. In practice, this dilemma is not very important, since one never really computes $R_{\mu\nu}{}^{i}$ and $P_{\mu\nu}{}^{q}$ but simply uses Eqs. (34) and (37) as estimates of the size of M^D+M^F. This is still a *valid* procedure if we remember that the $\omega_{1,2}\to 0$ limit of M^D+M^F must be cancelled by a correctly computed A^2 piece. The first nonvanishing piece in an expansion of M^D+M^F goes like $(\omega_{1,2}{}^2/E_G{}^2)\times(M^D+M^F)$. Thus, a reasonable "estimate" of the magnitude of the matrix element for Raman scattering in an empty crystal is obtained from Eqs. (33) and (35). At low frequencies, one takes the limit $\omega_{1,2}\to 0$ and multiplies by a factor $(\omega_{1,2}/E_G)^2$. At frequencies near the gap, we use Eqs. (33) and (35) directly.

C. Coupled Electron-Phonon System

Utilizing the results of Secs. III A and III B, it is possible to write (in terms of the quantities $R_{\mu\nu}{}^{i}$ and $P_{\mu\nu}{}^{q}$) the matrix element for the Raman scattering of light from the coupled electron-phonon system. We must consider separately the matrix elements for processes leading to an electron-hole–pair final state, Figs. 5 and 6, and those leading to a one-phonon final state, Fig. 8. The two distinct final states do not interfere with one another. In the discussion which follows we consider only the longitudinal-optic-mode phonon. This is the only mode which couples to the conduction electrons.

The electron-hole final state is computed using Figs. 5 and 6. Figure 5 gives a contribution which is unchanged relative to its value in the rigid lattice, Eq. (8). Figure 6 is essentially identical except for two rather minor changes. In addition to the bare Coulomb line (dashed line) characterized by φ, we may have a phonon line characterized by the "bare" phonon propagator

$$D(q,\omega)=2\omega_0/[(\omega-i\eta)^2-\omega_0{}^2]. \tag{38}$$

The vertex, instead of being purely Coulomb in character, may now have a phonon vertex as well, i.e., a

deformation potential or a Fröhlich-like coupling to the phonon or Coulomb line.

In the parabolic band approximation in a cubic crystal, the total matrix element (leading to a one-pair final state) to lowest order in the Coulomb and electron-phonon couplings is given by

$$M_{\mu\nu}^{\mathrm{EH}}=e_\mu{}^1 e_\nu{}^2\Big[\frac{m}{m^*}\delta_{\mu\nu}+\frac{m}{m^*}\delta_{\mu\nu}[\varphi_q+|V_q|^2D(q,\omega)]$$
$$\times[Q_e(q,\omega)+(m^*/m)\mathcal{E}]+\frac{\xi_{0q}{}^i k_l}{m}\Big(\frac{1}{2MN\omega_{0q}}\Big)^{1/2}$$
$$\times\tilde{R}_{\mu\nu}{}^i V_q D(q,\omega)+\frac{q\tilde{P}_{\mu\nu}{}^q}{m^2}[\varphi_q+|V_q|^2D(q,\omega)]\Big], \quad (39)$$

where V_q is given in Eq. (36). The quantities $\tilde{R}_{\mu\nu}{}^i$ and $\tilde{P}_{\mu\nu}{}^q$ are almost the same as their counterparts $R_{\mu\nu}{}^i$ and $P_{\mu\nu}{}^q$ defined in Eqs. (34) and (37) for the empty lattice. Both quantities are only weakly dependent on the presence of conduction electrons. The conduction electrons exclude (they occupy) a small set of states around the band minimum. The occupation of these states must be taken into account in the intermediate-state sums in, for example, Eq. (34). When the incident laser frequency is not very near the band gap, then it is clear that

$$\tilde{R}_{\mu\nu}{}^i=R_{\mu\nu}{}^i[1+O(\epsilon_F/E_B)].$$

When $\omega_{1,2}$ is near the direct band gap, the effective shift in the position of the singularity in $R_{\mu\nu}{}^i$ (energy denominator) must be taken into account. Loudon[11] has shown that near the direct band gap $R_{\mu\nu}{}^i$ is singular as $(E_g-\omega_{1,2})^{-1/2}$. The presence of conduction electrons shifts this singularity to the point $E_g+2\epsilon_F-\omega_{1,2}$.

In order to include the collective effects as in Sec. III A we merely divide the last three terms in Eq. (39) by

$$\epsilon_T(q,\omega)=1-[\varphi_q+|V_q|^2D(q,\omega)]Q_e(q,\omega). \quad (40)$$

The division by ϵ_T amounts to replacing the bare Coulomb plus bare phonon propagators in Fig. 6 by the heavy braided line (see Fig. 10). This geometric sum of bubbles is directly analogous to the set of diagrams summed in the pure Coulomb case (see Fig. 7). Taking the matrix element squared, summing over final states which conserve energy, and averaging over an initial ensemble at a temperature $\beta=1/kT$ as in Eq. (15), we get that portion of the scattering cross section for the coupled electron-phonon system which comes from an electron-hole–pair final state. In order to simplify the length of the algebraic expression somewhat, we consider the so-called perpendicular parallel scattering where the incident light is polarized along the x axis, the scattered light along the y axis, and the phonon along the z axis, where x, y, and z are the fourfold

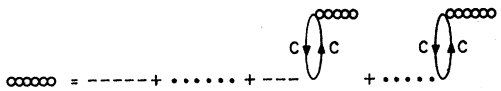

FIG. 10. Diagrammatic representation of the effective e-e interaction screened by the conduction electrons.

crystal axes. In this case

$$\frac{d\sigma(\perp,\|)}{d\omega\,d\Omega}\Big|_{\mathrm{EH}}=\frac{1}{\pi}r_0{}^2\frac{1}{1-e^{-\beta\omega}}$$
$$\times\Big|\frac{k_l}{m}\Big(\frac{1}{2MN\omega_{0q}}\Big)^{1/2}R_{xy}{}^z V_q D(q,\omega)$$
$$+qP_{xy}{}^z[\varphi_q+|V_q|^2D(q,\omega)]\Big|^2\frac{\mathrm{Im}Q_e(q,\omega)}{|\epsilon_T(q,\omega)|^2}. \quad (41)$$

The contribution to the scattering from the inclusion of a phonon final state is easily incorporated into our RPA type of approximation. The diagrams contributing to the matrix element are the same as those in Fig. 6, only the final state is changed. To zeroth order in the Coulomb interaction in the parabolic band approximation

$$M^{\mathrm{EP}}=e_\mu{}^1 e_\nu{}^2\Big[\delta_{\mu\nu}\frac{m}{m^*}V_q Q_e(q,\omega)$$
$$+\frac{\xi_{0q}k_l}{m}\Big(\frac{1}{2MN\omega_{0q}}\Big)^{1/2}\tilde{R}_{\mu\nu}{}^i+\frac{q\tilde{P}_{\mu\nu}{}^q}{m^2}V_q\Big]. \quad (42)$$

To include collective effects we divide Eq. (42) by the total dielectric constant, Eq. (40). The contribution to the cross section due to the phonon final state for the perpendicular parallel scattering is then

$$\frac{d\sigma(\perp,\|)}{d\omega\,d\Omega}\Big|_{\mathrm{EP}}=\frac{r_0{}^2}{\pi}\frac{1}{1-e^{-\beta\omega}}$$
$$\times\Big|\frac{k_l}{m}\Big(\frac{1}{2MN\omega_{0q}}\Big)^{1/2}R_{xy}{}^z+\frac{qP_{xy}{}^z}{m^2}V_q\Big|^2\frac{\mathrm{Im}D(q,\omega)}{|\epsilon_T(q,\omega)|^2}. \quad (43)$$

Mooradian and McWhorter[9] have arrived at a formula essentially identical to Eq. (41) for the total $(\perp,\|)$ cross section. Within strict RPA, $\mathrm{Im}D(q,\omega)$ is a δ function at the bare phonon frequency. For these values of q and ω, the dielectric constant $\epsilon_T(q,\omega)$ is proportional to a δ function squared, so that Eq. (43) is zero.[4] Thus, within the RPA, Eq. (41) gives the total $(\perp,\|)$ cross section.

In a real crystal there is a finite imaginary part to the propagator $D(q,\omega)$. The phonon lifetime arises from two distinct sources. The first and most obvious source is the coupling of the phonon to impurities, lattices defects, anharmonic terms, etc., in the *empty* lattice. The second mechanism for phonon lifetime is due to the

coupling of the phonon to the small number of conduction electrons present. In lightly doped crystals, the first mechanism will be the dominant one. Since the conduction electrons are treated within the RPA, the lifetime of the phonons due to the second mechanism is already included in Eq. (41), i.e., in $\mathrm{Im}Q_e$, and it would be inconsistent to include these effects a second time in ImD of Eq. (43). However, the lifetime effects attributable to the process not connected with the conduction electrons should, in a real case, be included in our equations.

We might conjecture that it is possible to include such finite lifetime effects by introducing a small phenomenological imaginary part to the phonon frequency, i.e., $\tau_{\mathrm{phonon}}^{-1}$. This is the procedure which gives the width and shape of the phonon line in the empty lattice.[11] It is also the procedure which properly gives the width and shape of the plasmon line and central ion line in the coupled electron-ion problem.[19] For the electron-phonon system there is a question as to whether it is consistent to use Eqs. (41) and (43) with a finite ImD. The difficulty comes from the fact that there is a possible double counting of mixed electron-phonon final states involved in such a procedure. This point is currently under investigation.

Assuming that we can neglect the contribution from Eq. (43), then we must make one further simplification in Eq. (41) before it reduces to Eq. (1) of Ref. 9. The simplification merely involves setting $[\varphi_q+|V_q|^2D(q,\omega)]Q_e(q,\omega)=1$ and $\varphi_qQ_e(q,\omega)=-\omega_p^2/\omega^2$. These approximations are valid only very near a resonance when the resonance is sharp enough and when we can neglect the dispersion of the plasmon, i.e., the deviation of φQ_e from $1-\omega_p^2/\omega^2$.

The results of this section, although algebraically quite complicated, are conceptually quite simple. The resonances in the total cross section will occur at the zeros of $\epsilon_T(q,\omega)$. The strength and polarization dependence of the resonances will depend on a detailed calculation of the quantities C, $\tilde{R}_{\mu\nu}{}^i$, and $\tilde{P}_{\mu\nu}{}^q$. The functional form of these objects will depend to a good approximation on the band structure of the solid and not on the presence of a small number of excess carriers. We can think of the experiments as giving us a means for determining the effective $R_{\mu\nu}{}^i$, $P_{\mu\nu}{}^q$, and perhaps the constant C.

IV. ZEROS OF THE DIELECTRIC CONSTANT

From our final expression for the cross section [Eqs. (41) and (43)], it is clear that the zeros of $\epsilon_T(q,\omega)$ determine the position of the resonances in the scattering cross section. Writing $\epsilon_T(q,\omega)$ explicitly by inserting $|V_q|^2$ from Eq. (36) into Eq. (40), we find

$$\epsilon_T(q,\omega)=1-\frac{4\pi e^2}{q^2\epsilon_\infty}Q_e(q,\omega)\frac{\omega^2-\omega_t^2}{\omega^2-\omega_l^2}. \tag{44}$$

Multiplying through by the quantity $(\omega^2-\omega_l^2)/(\omega^2-\omega_t^2)$, we see that the roots $\epsilon_T(q,\omega)=0$ are determined by[1,6]

$$0=\frac{\omega^2-\omega_l^2}{\omega^2-\omega_t^2}-\frac{4\pi e^2}{q^2\epsilon_\infty}Q_e(q,\omega). \tag{45}$$

In the absence of conduction electrons, $Q_e(q,\omega)=0$, the solution of Eq. (45) is $\omega=\omega_l$, the longitudinal-optic-mode frequency. For very high carrier concentration, i.e.,

$$(4\pi e^2/q^2\epsilon_\infty)Q_e(q,\omega)\to\infty\,, \tag{46}$$

the root of Eq. (45) is $\omega=\omega_t$, the transverse-optic-mode frequency.

In the neighborhood of the collective resonances, $qV/\omega\ll1$, so that, dropping all collisionlike terms,

$$\mathrm{Re}Q_e(q,\omega)=\frac{q^2n}{\omega^2m^*}\left[1+\frac{3q^2\langle V^2\rangle}{\omega^2}+\cdots\right]. \tag{47}$$

Here $\langle V^2\rangle=kT/m^*$ for a nondegenerate plasma at a temperature T and $\langle V^2\rangle=\frac{1}{5}V_F{}^2$ for a degenerate Fermi gas. The finite q effects in the expansion of the $\mathrm{Re}Q_e(q,\omega)$ will make themselves felt in the dispersion of the coupled plasmon-phonon line. This dispersion, which under typical experimental situations is of the order of a few percent, will manifest itself as an apparent shift of the Raman-scattered line as a function of temperature or angle of scattering.

The $\mathrm{Im}Q_e(q,\omega)$ can also be obtained in the limit $qV/\omega\ll1$. In the nondegenerate case, neglecting any effects due to impurities,

$$\mathrm{Im}Q_e(q,\omega)=\frac{n}{KT}(\tfrac{1}{2}\pi)^{1/2}\frac{\omega}{q\langle V\rangle}\exp\frac{-\omega^2}{2q^2\langle V^2\rangle}. \tag{48}$$

Physically, the imaginary part of $Q_e(q,\omega)$ in this "collisionless" case comes from the familiar Landau damping phenomenon, i.e., from electrons traveling at or very close to the phase velocity of the wave.

In the degenerate case, $\mathrm{Im}Q_e(q,\omega)$ would be equal to zero in the "collisionless" case, since there are no electrons around at the phase velocity ω/q. In a real material with impurities defects, etc., there is, in general, a finite imaginary part of $Q_e(q,\omega)$ which produces a broadening of any resonances and contributes to $\mathrm{Im}Q_e(q,\omega)$ for all ω/q. In some crude qualitative sense, these dissipative processes may be taken into account by letting $\omega\to\omega+i/\tau$, in the polarizability equation (14), where τ is scattering time. This scattering time is approximately equal to the time one gets from fitting the dc mobility data, i.e., $\mu\equiv e\tau/m^*$. It is assumed to be

[19] A. Ron, J. Dawson, and C. Oberman, Phys. Rev. **132**, 497 (1963); D. F. Dubois and V. Gilinsky, *ibid.* **133**, A1317 (1964).

frequency-independent. Tell and Martin,[20] working in GaAs, have observed a temperature dependence of the coupled plasmon-phonon linewidth which is in rough agreement with Eq. (48). The dispersion predicted by Eq. (47) was too small to be observed in that experiment.

APPENDIX

In this Appendix we show that the Raman cross section, in insulating crystals, will to a very good degree of approximation go like $(\omega_{1,2}/E_B)^4$ when $|\omega_{1,2}/E_B|\ll 1$. The "proof" depends on rather general considerations. It is valid within the framework of the BOA as long as the excited state, which the system is left in after the scattering is low in energy relative to typical electronic energies in the crystal.

It is well known[21] that the electronic polarizability, or, equivalently, the matrix element for the elastic scattering, of light, goes like $(\omega_{1,2}/E_B)^2$ at low frequencies. The Raman scattering differs from the elastic scattering in that the final and initial states of the system differ from one another. We will show that the small amount of inelasticity involved in the Raman process, i.e., the excitation of a phonon, is irrelevant. It is only the electronic energies which are relevant to a discussion of the frequency dependence of the Raman scattering cross section.

The matrix element to second order in the electromagnetic field for the scattering of light is given by

$$M=e_\mu{}^1 e_\nu{}^2\left\{\langle f|A^2|i\rangle\delta_{\mu\nu}+\sum_l\left[\frac{\langle f|P_\nu A^*|l\rangle\langle l|P_\mu A|i\rangle}{E_i-E_l+\omega_1}+\frac{\langle f|P_\mu A|l\rangle\langle l|P_\nu A^*|i\rangle}{E_i-E_l-\omega_2}\right]\right\}, \quad \text{(A1)}$$

where

$$A^2=\sum_i e^{i\mathbf{q}\cdot\mathbf{x}_i}$$

and

$$P_\mu A=\sum_i P_\mu{}^i e^{i\mathbf{k}_1\cdot\mathbf{x}_i},$$

$$P_\nu A^*=\sum_i P_\nu{}^i e^{-i\mathbf{k}_2\cdot\mathbf{x}_i}.$$

When $i=f$ and $\omega_{1,2}\to 0$, the sum of the last two $\mathbf{P}\cdot\mathbf{A}$ terms in Eq. (1) cancel exactly with the first term. This is the content of the so-called f sum rule.[21] In an insulating crystal, the wave function in the BOA may be written

$$\psi=\sum_{n,m}\varphi_n(\mathbf{x},\mathbf{R})H_m{}^n(\mathbf{R}), \quad \text{(A2)}$$

where the vector $x\equiv(\mathbf{x}_1,\cdots,\mathbf{x}_M)$ specifies the electronic coordinates and $R\equiv(\mathbf{R}_1,\cdots,\mathbf{R}_N)$ the nuclear coordinates. The index n specifies the nth electronic configuration and m the vibrational state of the system. In the Raman process n does not change, i.e., it remains in the $n=0$ state. The vibrational state will, of course, change.

Let us look at the A^2 piece of Eq. (A1) and rewrite it. The procedure we adopt is the exact analog of what one does in the single isolated atom case where one takes nuclear recoil into account. We find

$$\begin{aligned}\delta_{\mu\nu}&\langle f|A^2|i\rangle\\ &\equiv\delta_{\mu\nu}\langle\varphi_0(x,R)H_m{}^0(R)|\sum_i e^{i\mathbf{q}\cdot\mathbf{x}_i}|\varphi_0(x,R)H_0{}^0(R)\rangle\\ &\equiv\delta_{\mu\nu}\langle\varphi_0(x,R)H_m{}^0(R)|\\ &\qquad\times\sum_{i,j}e^{i\mathbf{q}\cdot(\mathbf{x}_i-\mathbf{R}_i)}e^{+i\mathbf{q}\cdot\mathbf{R}_j}|\varphi_0(x,R)H_0{}^0(R)\rangle. \quad \text{(A3)}\end{aligned}$$

The $e^{i\mathbf{q}\cdot(\mathbf{x}_i-\mathbf{R}_i)}$ factor may be set equal to 1, since in the integration over the electrons' coordinates the spread in the electrons' wave function away from any given ion site is much smaller than the wavelength of the light. A simple uncertainty-principle argument—to wit, that the gap energy E_g, i.e., the "binding energy," of the electron roughly determines the spread of the electrons' wave function in real space—implies that neglecting q in the exponent is good to terms of order $q(\hbar c/E_g)$. The $\sum_i e^{i\mathbf{q}\cdot\mathbf{R}_i}$ may *not* be set equal to 1 in the integral over the nuclear coordinates; thus,

$$\delta_{\mu\nu}\langle f|A^2|i\rangle=\delta_{\mu\nu}\langle H_m(R)|\sum_i e^{i\mathbf{q}\cdot\mathbf{R}_i}|H_0(R)\rangle. \quad \text{(A4)}$$

The total matrix element, Eq. (A1), in this approximation is

$$\begin{aligned}M=e_\mu{}^1 e_\nu{}^2&\langle H_m(R)|\sum_i e^{i\mathbf{q}\cdot\mathbf{R}_i}|H_0(R)\rangle\\ &\times\left(\frac{1}{m}\sum_n\left[\frac{\langle 0|P_\nu|n\rangle\langle n|P_\mu|0\rangle}{E_n-E_0-\omega_1}+\frac{\langle 0|P_\mu|n\rangle\langle n|P_\nu|0\rangle}{E_n-E_0+\omega_2}\right]+\delta_{\mu\nu}\right). \quad \text{(A5)}\end{aligned}$$

In Eq. (A5), we have neglected any dependence of the intermediate-state energies on the phonon energies. The theorem, i.e., the frequency dependence of M, follows directly from the conventional f sum rule on the electronic part of the wave function alone.

[20] B. Tell and R. Martin, Phys. Rev. (to be published).
[21] W. Heitler, *Quantum Theory of Radiation* (Clarendon Press, Oxford, 1954), p. 34.